Shape and size dependent bactericidal activity of photoirradiated TiO_2 nanostructures

A

Thesis

Submitted in partial fulfillment for the award of the

Degree of

Masters of Science in Biotechnology

By

Gunveen Wadhwa

Registration No. 300901028

Under the Supervision of

Dr. Bonamali Pal

Assistant Professor

School of chemistry & Biochemistry

Thapar University, Patiala

Dr. Niranjan Das

Associate Professor

Dept. of Biotech. & Env. Sciences

Thapar University, Patiala

Department of Biotechnology & Environmental Sciences

Thapar University, Patiala

July 2011

Certificate

This is to certify that the project entitled **"Shape and size dependent bactericidal activity of photoirradiated TiO_2 nanostructures"** being submitted by Ms. Gunveen Wadhwa in partial fulfillment of the requirement for the award of degree for the Master of Science in the Department of Biotechnology and Environmental Sciences, Thapar University, Patiala, is a bonafide work carried out under our guidance and supervision and that no part of this project has been submitted for the award of any other degree.

Dr. Bonamali Pal
Assistant Professor
SCBC, Thapar University, Patiala

08/07/2011
Dr. Niranjan Das
Associate Professor
DBTES, Thapar University, Patiala

Dr. M. S. Reddy
Head of Department
DBTES, Thapar University, Patiala

Dr. S. K. Mohapatra
Dean, Academic Affairs
Thapar University, Patiala

Candidate's Declaration

I hereby declare that the work which is being presented in the dissertation entitled **"Shape and size dependent bactericidal activity of photoirradiated TiO_2 nanostructures"** in partial fulfillment of the requirements for the award of the degree of Master in Science in Biotechnology, Department of Biotechnology and Environmental Sciences, Thapar University, Patiala is an authentic record to my own work during a period of 6 months from Jan 2011 to Jun 2011, under the supervision of Dr. N. Das, Department of Biotechnology and Environmental Sciences and Dr. Bonamali Pal, School of Chemistry and Biochemistry, Thapar University, Patiala. I have not submitted the matter embodied in this dissertation for the award of any other degree or diploma.

Gunveen Wadhwa

Patiala
Date: 8 July, 2011

This is to certify that the above statement given by the candidate is correct and true to the best of our knowledge.

Dr. Bonamali Pal
Assistant Professor
School of Chemistry and Biochemistry

08/07/2011

Dr. Niranjan Das
Associate Professor
Dept.of Biotech. and Env. Sciences

Acknowledgement

Words often fail to express one's inner feeling of indebtedness. It is difficult to enunciate in words the deep sense of gratitude which I have for my esteemed supervisor Dr. Bonamali Pal, Assistant Professor, School of Chemistry and Biochemistry and Dr. N. Das, Associate Professor, Department of Biotechnology and Environmental Sciences, Thapar University, Patiala, for their support and patience. Their invaluable assistance and precious guidance helped me in executing this arduous task from its conception to it completion.

I take this opportunity to thank Mr. Raghavendra Aminedi, research scholar for his guidance, critical and timely suggestions and immense encouragement. I also have deep gratitude towards him for never turning down any query. I thank Mr. Inderpreet Singh, Mr. Rohit Singh, Ms. Nidhi Gupta, Ms. Mahiti Gupta, Mr. Vinit Meshram, Ms. Neha Kapoor, research scholars in Chemistry and Biotechnology Department for their kind cooperation during the project work. I would specially thank Mr. Kunal Garg for his kind help.

It has been a memorable two year time in Thapar University with friends like Banpreet, Sonal, Karnika, Amit, Ravinder and Nidhi. Last but not the least, I would like to thank the faculty members and Dr. M. S. Reddy, Head, Department of Biotechnology and Environmental Sciences, Thapar university, Patiala, my family and friends who supported me and encouraged me to work hard, without which this could not have been possible.

Gunveen Wadhwa

DEDICATED TO MY MOTHER.....

ABSTRACT

The most widely used anatase-TiO_2 (P25, Degussa, Germany, size 30-50 nm) photocatalyst of spherical shape has been found to display high bacterial killing effect under UV light irradiation. The mechanism involves the production of electron-hole (e-h+) pair by the photoexcited TiO_2, which are responsible for the oxidation and reduction of the adsorbed species on the TiO_2 surface and the strongly oxidizing positive holes decompose the bacterial cells. Recently it has been discovered that the photocatalytic activity of TiO_2 is significantly changed with change in size, shape and surface structural morphology. However, till date, there are no reports available in the literature about the bacterial killing effect of different shapes of TiO_2 nanostructures. To our knowledge, this is the first report about the comparative bactericidal activity of different shapes of TiO_2 nanoparticles. In this work, we prepared TiO_2 nanosphere, nanorod and nanotube, characterized their surface structural dissimilarity and finally investigated their photocatalytic antibacterial properties with respect to killing of prokaryotic gram-negative bacterium *Agrobacterium tumefaciens* LBA4404. The effect of Au, Ag and Cu co-catalysts photodeposition onto TiO_2 for the enhanced photokilling efficiency and their relative co-catalytic activity was also verified.

The XRD structural study, TEM size & shape analysis and surface area measurement confirmed the formation of TiO_2 spherical (size = 30-50 nm & surface area = 55 m^2/g), nanorod (length = 90-114 nm, width = 8.1-11.5 nm, aspect ratio = length/width = 8.5-13.5 & surface area = 69 m^2/g) and nanotube (length = 93- 118 nm, width = 9.8-15 nm, aspect ratio = 6.99-13.66 & surface area = 176 m^2/g) crystal structure and surface morphology. It has been found that TiO_2 nanotube and nanorod showed higher bactericidal activity than spherical shape particles. The TiO_2 nanotube displayed highest bacterial killing effect because of its highest surface area (176 m^2/g) & surface to volume ratio (0.32-0.44 nm^{-1}) among the studied photocatalysts. The Au and Ag deposited TiO_2 nanoparticles exhibited better efficiency in bacterial death as compared to Cu loading and bare TiO_2 photocatalysts. This difference in antimicrobial properties can be explained on the basis of their structural morphology & surface area difference, variation in energetics of photoexcited charge species, photogenerated electron transfer rate and their redox ability. Atomic Absorption Spectroscopy elemental analysis also confirmed the potassium ions, K^+ leakage during photocatalytic killing of bacterial cells during light illumination over TiO_2 nanostructures.

TABLE OF CONTENTS

1. Introduction

Nanotechnology is a deliberate manipulation of matter at size scales of less than 100 nm that holds the promise of creating new materials and devices which take advantage of unique phenomena realized at those length scales. Nanoparticles (NPs) exhibit significantly novel and improved physical, chemical, optical and biological properties, and functionality due to quantum size effect. These are attracting a great deal of attention because of their potential applications for achieving specific processes and selectivity, especially in biological and pharmaceutical applications. Discoveries in the past decade have demonstrated that the optical and catalytic properties of noble-metal and semiconductor nanocrystals are highly influenced by their shape and size.

With the outbreaks of infectious diseases caused by pathogenic bacteria and the rise of antibiotic resistance of bacteria, much attention in pharmaceutical and medical fields has been focused on creating new antibacterial agents. Recent studies have demonstrated that specially formulated metal oxide NPs have good antibacterial property, and thus antimicrobial formulations comprising NPs could be used as effective bactericidal materials. Many kinds of nanosized antibacterial materials such as TiO_2, ZnO, MgO, chitosan, calamine, copper and silver have been reported in this area. The most active photocatalyst is the TiO_2 anatase crystal phase, and most work has been done using the P25-TiO_2 produced by Degussa Chemical Company (Germany). This material is a mixture of phases with an approximate composition of 75% anatase and 25% rutile whose particle size and surface area are 30-50 nm and ~55 m^2/g respectively. Numerous investigations have reported that the addition of noble metals such as platinum, silver, or palladium may enhance the overall photoefficiency of TiO_2. This effect is almost conclusively attributed to a reduction in the recombination rate due to better charge separation between the electrons, which accumulate on the metal, and the holes, which remain on the photocatalyst surface.

1.1 Principles of TiO_2 photocatalysis

Photocatalysis is an "acceleration of a chemical reaction in the presence of light". The semiconductor photocatalytic process is reported to occur via the absorption of a photon of energy equal to or greater than the semiconductor band gap energy. Most current research reported on photocatalysis is using TiO_2 whose band gap energy is 3.2 eV. The photocatalytic process includes chemical steps that produce reactive species that in principal can cause fatal damage to

microorganisms. When TiO_2 particles are irradiated with near UV irradiation (> 350 nm), electron–hole pairs are generated on the photocatalyst surface.

On semiconductors such as titanium dioxide, however, they survive for longer periods of time. The ratio of the recombination rate (between electrons and holes) to the rate of production of electron-hole pairs is a good indicator of the maximum efficiency of a photocatalytic reaction. One of the notable characteristics of titanium dioxide is that the oxidizing power of the hole is greater than the reducing power of the excited electrons. On the surface of the catalyst, there is approximately a single layer of tightly adhering (adsorbed) water molecules. When these adsorbed water molecules are oxidized by holes, hydroxyl radicals (OH.), which have strong oxidizing power are formed. The hydroxyl radicals can then react with organic compounds, initially producing free radicals. Meanwhile, the electrons photogenerated are also used to reduce oxygen in the air, producing the superoxide radical anion (O^{2-}) and ultimately converted to hydrogen peroxide and hydroxyl radicals. Thus both positive holes and OH radical can decompose all the adsorbed organics to CO_2 and H_2O. This photooxidation rate changes with size and shape of photocatalyst due to the change in band gap energy in relation to CB and VB location, hence the photoredox ability as shown below.

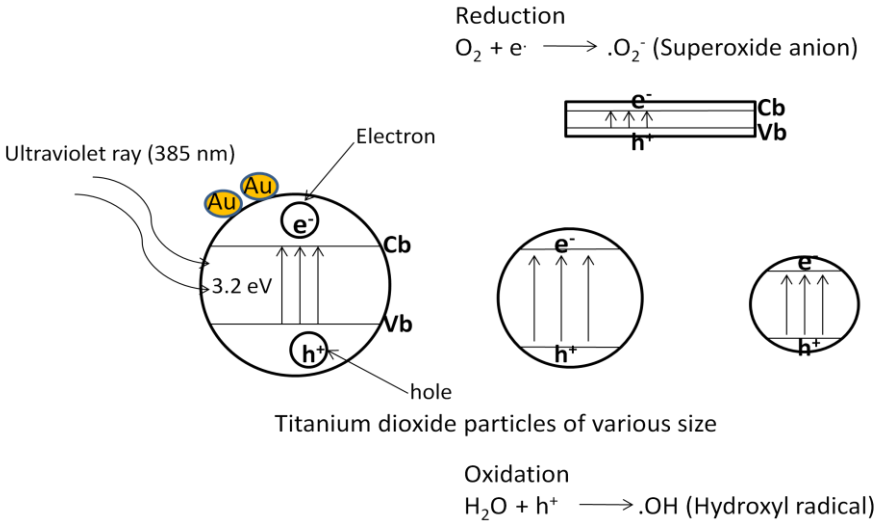

Figure 1. Photocatalytic reaction mechanism of irradiated TiO_2 of different shapes and sizes.

1.2 Function of metal loading

Metal loading is mainly done in order to improve the photocatalytic activity of TiO_2. The photocatalytic activity of TiO_2 is observed to be very poor in the absence of a metal. Generally a noble metal like Pt, Pd, Rh, Au or Ag is deposited to the surface of TiO_2 in order to avoid the

recombination of electron and hole pairs because the deposited metal picks up the photoexcited electron and thereby free hole takes part in oxidation reaction more rapidly. Only when this recombination is prevented the photocatalytic activity can be enhanced and redox reactions can be easily carried out. The rate of electron transfer from TiO_2 to metal depends on electronegativity, work function of metal and size & shape of the deposited metal. The TiO_2 offers great potential as a bactericidal agent because of the following properties:-

1. ***Sunlight or Direct UV light exposure*** enhances the rate of reaction.
2. Oxidation of the substrates to $\boldsymbol{CO_2}$ is complete.
3. The photocatalyst is ***inexpensive*** and has a high turnover.
4. Does not get rusted.
5. TiO_2 can be supported on ***suitable reactor substrates***
6. Reusable

1.3. Target bacterial cells

Bacteria are prokaryotic microorganisms that do not contain nucleus which is characteristic of cells of higher plants and animals (eukaryotic cells). The DNA molecules do not have a nuclear membrane to separate them from the cytoplasm. The cytoplasm of prokaryotic cells is not differentiated into distinguishable units for specialized functions; for example, respiration takes place on the cell membrane. Although there are thousands of different species of bacteria, most of them fall into three general morphologies: spherical, rod or spiral. Their size ranges from 0.5 to 5 microns in maximum dimensions. Based on the different ability of their cell wall components to be stained by the Gram stain, bacteria are divided into two classes: Gram-positive and Gram negative organisms.

The bacterium of interest for our studies is Gram negative *Agrobacterium tumefaciens*. The cell wall of the Gram-negative cells is chemically more complex. Here the peptidoglycan layer is thinner (2-6 nm thickness) and accounts for only 10% of the cell wall. The outermost layer of Gram-negative bacteria, the outer membrane, is about 6 to 18 nm thick and accounts for the rest of the cell wall. The outer membrane consists of 50% lipopolysaccharides, 35% phospholipids and 15% lipoproteins.

***Agrobacterium tumefaciens*:**

Agrobacterium tumefaciens is a rod shaped Gram negative soil bacterium (Smith *et al*., 1907). It belongs to the family Rhizobiaceae, which includes the nitrogen fixing legume symbionts. Unlike the nitrogen fixing symbionts, tumor producing *A.tumefaciens* are parasitic and do not benefit the plant. The wide variety of plants affected by *A.tumefaciens* makes it of great concern to the agriculture industry. Economically, *A.tumefaciens* is a serious pathogen of grapevines, stone fruits, nut trees etc. and therefore acts as a model organism to be studied, to elucidate the mechanism of photocatalysis.

2. Literature Review

Much work has been done in past by various scientists on anti-microbial activity of TiO_2 taking *Lactobacillus acidophilus, Saccharomyces cerevisiae, Pseudomonas aeruginosa, Salmonella cholerasuis, Vibrio parahaemolyticus, Bacillus subtilis, and Escherichia coli* etc. as subject microbes. But till date, there are no reports available in the literature about the effects of different shapes of TiO_2 NPs on bacterial killing. In the present study, antibacterial activity of different shapes and coinage metal loaded TiO_2 has been checked on *Agrobacterium tumefaciens*. Some of the literature related to the present study has been cited below:

Matsunaga *et al*; reported the novel concept of photochemical sterilization. They killed microbial cells photoelectrochemically with semiconductor powder (platinum-loaded titanium oxide, TiO_2/Pt). Coenzyme A, (CoA) in the whole cells was photo-electrochemically oxidized and, as a result, the respiration of cells was inhibited. They also reported photochemical sterilization system in which E.coli cells were sterilized with photosemiconductor powders (titanium oxide) and they found this system to be reusable.

M. Cho *et al*; demonstrated that the concentration of OH radicals and the biocidal activity in TiO_2 photocatalytic disinfection is linearly co related. These results indicated that the OH radical is the primary oxidant species responsible for inactivating E.coli in the UV/TiO_2 process. Also, investigation of different inactivation behaviors of MS-2 phage and *E.coli* upon action of TiO_2 photocatalyst was carried out by them. They concluded that MS-2 phage is inactivated mainly by the free hydroxyl radical in the solution bulk but *E.coli* is inactivated by both the free and the surface-bound hydroxyl radicals.

S. Banerjee and co-workers visualized photocatalytic bactericidal activity of TiO_2 using Atomic Force Microscopy and discussed various reactions involved in production of reactive oxygen species and hydroxyl radical to understand the process involved in photocatalytic biocidal activity.

I. C. Mccullagh *et al*; presented a review which summarized recent developments concerned with the photocatalytic treatment of water contaminated with pathogenic micro-organisms.

K. Sunada and co-workers; elucidated the mechanism for photokilling of *E.coli* cells on TiO_2 thin films. They showed that the photokilling reaction is initiated by a partial decomposition of the outer membrane, followed by disordering of the cytoplasmic membrane, resulting in cell death.

C. C. Trapalis *et al*; prepared TiO_2 based nanostructured Fe^{3+} doped coatings by sol-gel method on glass substrates. These coatings exhibited a high antibacterial activity, which was enhanced with the increase of the temperature of thermal treatment and formation of anatase crystalline structure.

Pin-Ching *et al*; gave evidence for the first time that lipid peroxidation reaction is the underlying mechanism of death of *Escherichia coli* K-12 cells that are irradiated in the presence of the TiO_2 photocatalyst. They concluded that TiO_2 photocatalysis promoted peroxidation of the polyunsaturated phospholipid component of the lipid membrane initially and induced major disorder in the *E. coli* cell membrane.

K. Peter *et al*; investigated reactive magnesium oxide NPs and halogen (Cl_2, Br_2) adducts of these MgO particles and allowed them to contact certain bacteria and spore cells. Bacteriological test data, atomic force microscopy (AFM) images and electron microscopy (TEM) images were provided which yielded an insight into the biocidal action of these nanoscale materials.

Lidia Armelao and team members; worked on the photocatalytic performances and antibacterial activity of TiO_2 and Au/TiO_2 nanosystems. The photocatalytic performances of the obtained nanosystems in the elimination of *Bacillus subtilis* were illustrated and discussed in comparison with films obtained from standard Degussa P25 powders.

Chun Hu *et al*; investigated the photocatalytic disinfection of pathogenic bacteria in water with AgI/TiO_2 under visible light (*ì > 420 nm)* irradiation. The catalyst was found to be highly effective in killing *Escherichia coli* and *Staphylococcus aureus.*

Sukdep Pal and co-workers; investigated the antibacterial properties of different shapes of silver NPs against the gram negative bacterium *Escherichia coli*, both in liquid systems and on agar plates.

Dong Suk Kim and Seung-Yeop Kwak; investigated photocatalytic inactivation of *E.coli* with the film adhesion method by using Degussa P25 TiO_2 and mesoporous TiO_2 coated on glass. They found that the efficacy of photocatalytic disinfection with the film adhesion method is strongly

dependent on the surface area and crystallite size: the larger the surface area and the smaller the crystallites, the higher the efficacy of the photocatalytic inactivation.

Qi Li *et al*; synthesized nitrogen doped Titanium oxide by a sol gel process for disinfection using *E.coli* as target bacteria. They showed that the calcination atmosphere has strong effects on the composition, structural, optical and antimicrobial properties of TiON NPs. They concluded that C-TiON composite photocatalyst has a much better photocatalytic activity than pure TiON photocatalyst under visible light illumination.

Kayano Sunada and co-workers; examined the antibacterial effect for a thin transparent TiO_2 film and the photocatalytic degradation of endotoxin (a pyrogenic constituent of *E.coli*). They showed that the TiO_2 photocatalyst has both bactericidal activity and decomposing activity for the endotoxin (i.e. detoxifying activity).

Zhe-Xue-Lu and team members; investigated the bactericidal mechanism of TiO_2 by AFM in conjugation with some other techniques. They examined the dependence of the permeability of the cell membrane and cell viability on the stepwise cell wall and cell membrane damages. They concluded that decomposition of cell walls and cell membranes caused by an illuminated TiO_2 thin film may be the reason for cell death.

A. D. Belapurkar *et al*; prepared high surface-area TiO_2 photocatalysts supported on a glass tube and a stainless steel plate and evaluated for their bactericidal effect using water primed with *Escherichia coli*, in a quartz reactor using 350 nm light and solar light. They found that *E. coli* concentration decreased to a safe level from initial concentration of 500–100,000 bacteria/ml during 4 h of photolysis using 350 nm light and solar light. Time required for disinfection of water was found to increase with increase in the concentration of bacteria.

3. Objectives of the present study

As found in the literature TiO_2 has drawn attention by many researches for its wide applications both as photocatalyst and as bactericidal agent. However, there are no reports in the literature regarding the size and shape dependent antimicrobial activity of TiO_2 NPs and the metal loading effects. As metal loaded TiO_2 is more effective than bare TiO_2 as found in traditional photoreactions, it is interesting to study the effect of metal loading on these different shaped TiO_2 for bacterial killing. Keeping in view, the following objectives are framed accordingly.

- Synthesis and characterization TiO_2 NPs having different shapes
- To compare the bactericidal activity of differently shaped TiO_2 NPs
- To investigate the influences of Au, Ag and Cu loading onto TiO_2 for the enhancement of bactericidal activity

4. Experimental methods

4.1 Materials: All chemical were used without further purification

NaOH (Loba Chemie), HNO_3 (Loba Chemie), Isopropyl alcohol (Loba Chemie), $HAuCl_4.3H_2O$ (Sigma Aldrich), $AgNO_3$ (Fisher Scientific), $Cu(NO_3)_2$ (Loba Chemie) , NaCl (Loba Chemie). All the glassware and plasticware were procured from Borosil India Ltd., and Tarsons Private Ltd. All the glasswares and materials [Conical Flask (250 ml, 500 ml), Test tubes, tips, oakridge tubes] used in the experiment were autoclaved at 121°C for 15 min to ensure sterility.

Chemical composition of YEM media (g/l)	
Yeast Extract	0.4
D-Mannitol	10
$MgSO_4.7H_2O$	0.2
K_2HPO_4	0.5
NaCl	0.1
Agar	15

4.2 Synthesis of different TiO_2 nanoparticles

Spherical: The spherical TiO_2 NPs used in our study was a commercially available TiO_2 (P-25), Degussa Company Ltd., Germany. It consists of ~75% anatase and ~25% rutile with a average particle size of 30-50 nm and surface area 54 m^2/g.

Nanotube: 5 g of the P25-TiO_2 was mixed with 70 ml of 10N NaOH solution and subjected to hydrothermal treatment at 130^oC in a Teflon lined autoclave for 20 h. After this treatment, the filtered sample was washed with different amounts of 0.1 N HNO_3 and finally by methanol to give nanotube suspension. This suspension was then dried at 70^oC for 3 hrs to get the final product as nanotubes.

Nanorod: Taking the above produced nanotube as precursor, slurry was made in water at pH 5.6. This was then subjected to hydrothermal treatment in the autoclave at 175^oC for 48 h. The resulting slurry then initially washed with water and then finally with methanol to get nanorods as the end product.

Metal loaded nanoparticles: 50 mg of TiO_2 (spherical/rod/tube) was taken in a test tube containing magnetic bead and 5 ml of 50% V/V IPA (Isopropyl alcohol) was added along with the required amount of metal salt [$HAuCl_4.3H_2O$, $AgNO_3$, $Cu(NO_3)_2$]. Then Argon purging was done for 15 min which was then irradiated under UV light (125 W Hg arc lamp) for 2 hrs. After this treatment, the sample was washed with water and then finally with methanol to get the metal loaded NPs as final product which were dried at 70^{o}C for 30 min.

4.3. Culture of microorganisms

A.tumefaciens LBA4404 strain was aerobically grown in 25 ml of YEM broth at 28°C on a rotary shaker (120 rpm) for 20 hrs till the absorbance reached 0.9 at 660 nm wavelength. *A.tumefaciens* LBA4404 cells were harvested by centrifugation at 6500 rpm for 10 min, washed and suspended in 0.9% saline (5 ml).

4.4. Preparation of slides

Slides with different concentrations of

- Bare and metal loaded P25 Degussa titanium dioxide
- Bare and metal loaded nanorod titanium dioxide
- Bare and metal loaded nanotube titanium dioxide

First the glass slides were completely sterilized with alcohol. 100 µl of distilled water was put on the slide in the form of a drop. Known amounts of bare and metal loaded spherical, nanorod, nanotube TiO_2 NPs were weighed and added to the drop on different slides. Then the slides were transferred to hot plate (maintained at 80°C). Using a spatula the solution of TiO_2 was mixed and evenly spread, covering an area of 2×2.5 cm^2. The slides were allowed to dry for 15 min. Then all the prepared slides were transferred to a beaker and the beaker along with slides was kept in oven maintained at 200°C, for 2 hours. This ensured proper immobilization of NPs on slide as well as complete sterilization. The beaker was opened only in laminar air flow for further use of slides.
In this way, slides of amounts: 1mg and 0.5 mg were prepared.

4.5. Procedure

i) NPs were coated on a sterile glass slide to form thin films and immobilized in oven at 200^{o}C.

ii) *A.tumefaciens* is grown in YEM broth at 28^{o}C overnight in a shaker and the cells were harvested through centrifugation.

iii) The cells (*A.tumefaciens)* were suspended in 5 ml of 0.9% saline solution. From this cell suspension, dilutions up to 10^{-3} were made.

iv) 100 µl from this 10^{-3} dilution were spread on each NP coated slide and exposed to UV for different time periods.

v) The activities of variously shaped TiO_2 particles on bacterial cells were checked under long UV wavelength (having intensity of 6.4 W/m^2 at a distance of 5.5 cm.)

vi) After UV exposure, cell suspension was poured into eppendorff tube and 100 µl of cells were plated on to YEM agar plates containing streptomycin (50 µg/ml) and rifampicin (15 µg/ml).

vii) The plates were incubated at 28°C for 48 hours and the number of colonies on the plates were counted.

vii) The photocatalytic mechanism and the contents released from the cells were analysed through Atomic Absorption Spectroscopy

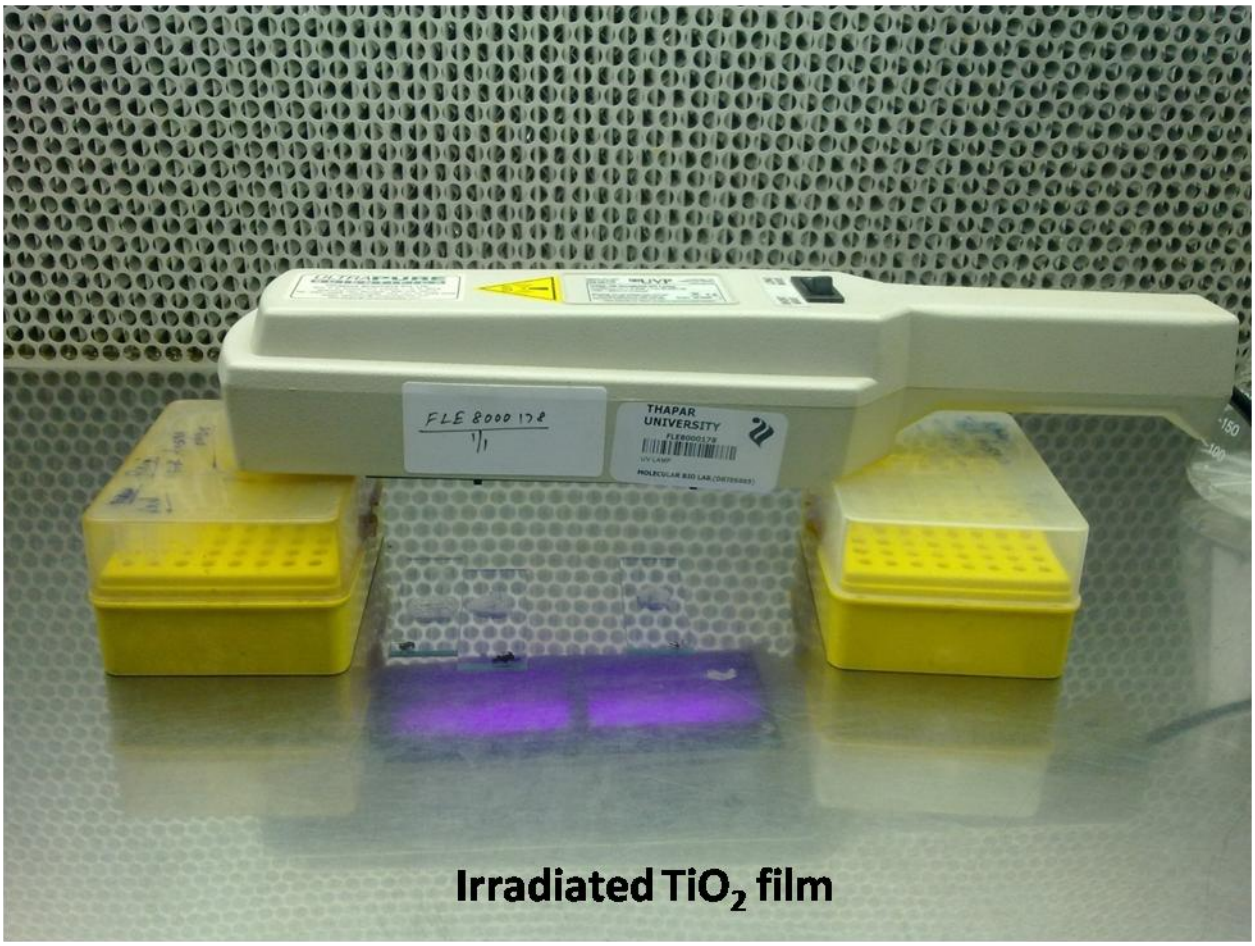

Figure 2. Irradiation (UV torch) of bacterial suspensions over TiO_2 coated glass slides

4.6. Procedure for Atomic Absorption Spectroscopy

For understanding the photocatalytic mechanism, Atomic Absorption Spectroscopy was carried out to check the potassium ion K^+ leaching from dead bacterial cells. 100 mg/ml of nanotube Au 1% 0.5 mg was prepared in sterile double distilled water. From this, 75 µl was added to 15 ml of saline containing bacterial culture to obtain a working concentration of 0.5 mg/ml NPs. The bacterial suspension was irradiated for 5 min with continuous stirring. The bacteria and the NPs were settled by centrifugation at 6500 rpm for 10 mins. The supernatant was analysed by AAS to check for the amount of potassium ions released from the bacteria.

5. Results and discussion

5.1. Characterization of nanoparticles

The XRD structural study, TEM size & shape analysis and surface area measurement confirmed the formation of TiO_2 spherical, nanorod and nanotube crystal structure and surface morphology.

Figure 3. shows the TEM images of 1wt% Au and Ag photodeposited TiO_2 nanospheres of size = 30-50 nm and surface area = 55 m^2/g.

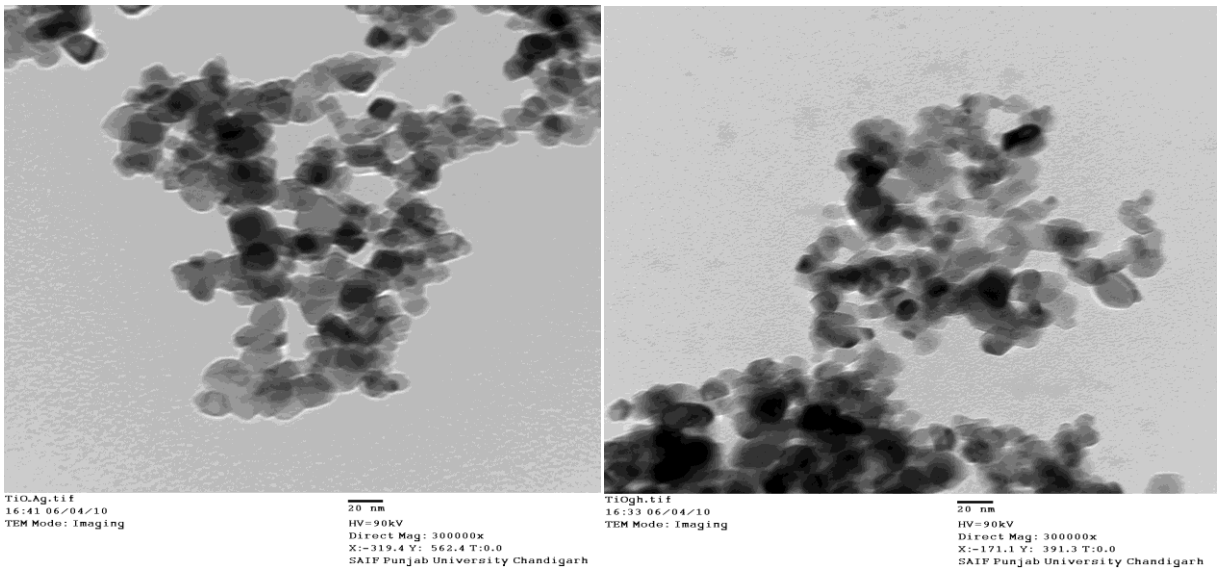

Figure 3. TEM images of 1 wt% (a) Au and (b) Ag deposited TiO_2 nanospheres.

It can be seen that some black colored aggregated nanodeposits of Au and Ag on the spherical shape grey TiO_2 NPs and not all the particles are covered with metals. The SEM surface morphology of TiO_2 nanorod shown below looks like aggregated nanorod assemblies.

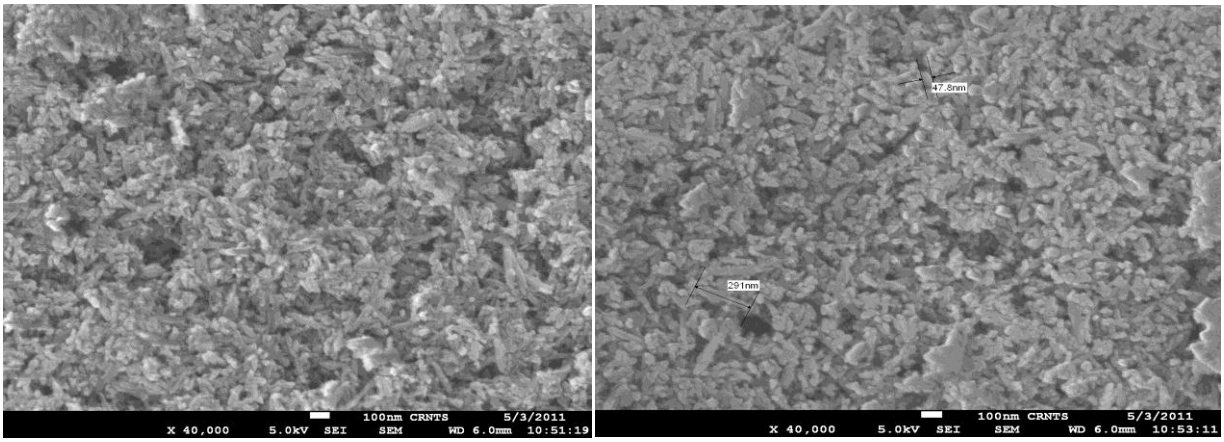

Figure 4. SEM surface morphology of TiO_2 nanorods

Figure 5. represents the TEM images of TiO_2 nanorods. Very fine rod shaped nanocrystals of length = 90-114 nm, width = 8.1-11.5 nm, aspect ratio = length/width = 8.5-13.5 and surface area = 69 m^2/g are seen in the images.

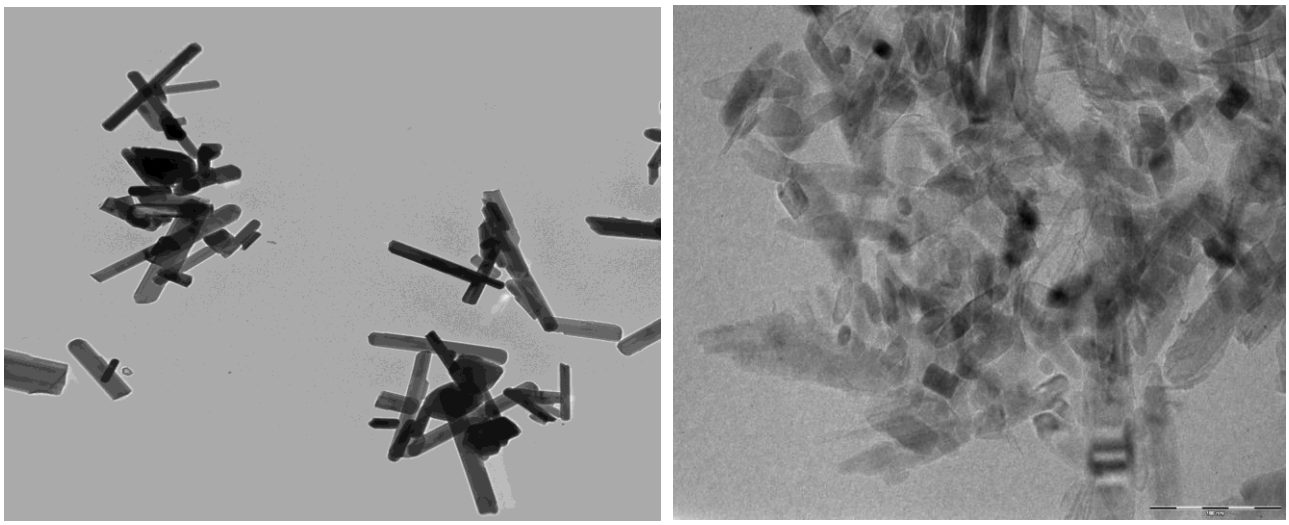

Figure 5. TEM images of TiO_2 nanorods.

The TEM images of lengthy hollow straw like structures of TiO_2 nanotubes of length = 93-118 nm, diameter = 9.8-15 nm, aspect ratio = 6.99-13.66 and surface area = 176 m^2/g are shown in figure 6. Many hollow tubes are seems to be aligned randomly. The higher surface area also represents that this TiO_2 nanostructures have hollow interior as compared to solid nanorods of having lesser surface area 69 m^2/g.

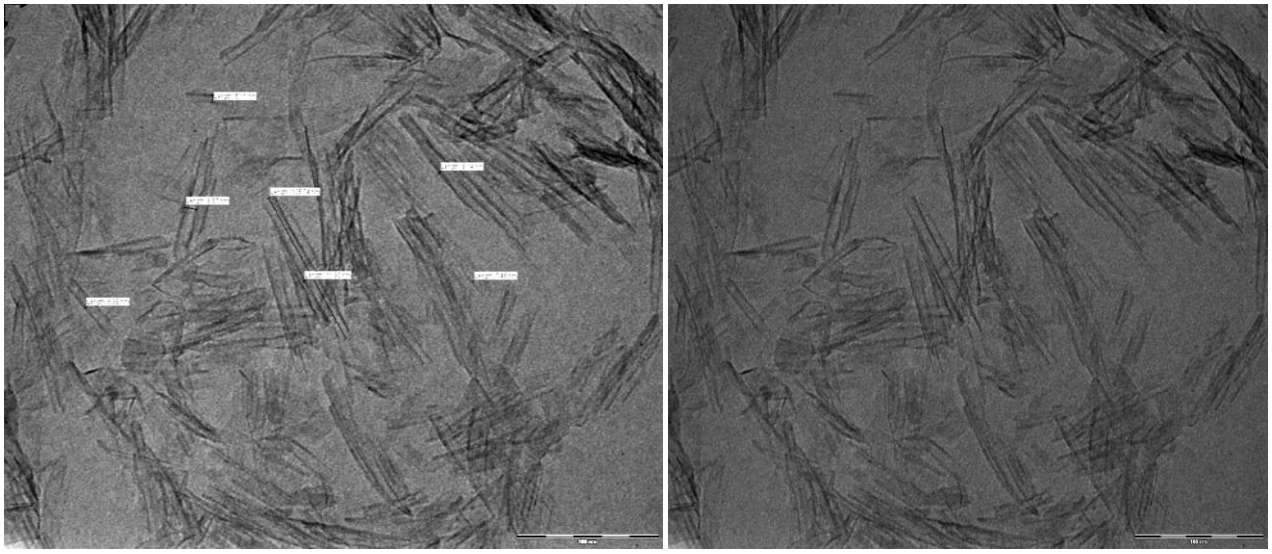

Figure 6. TEM images of TiO_2 nanotubes

5.2 Photocatalytic bacterial killing by bare TiO_2 nanoparticles

In order to study the bacterial photocatalytic killing, different bare NPs were used in the present study which are of different shape viz. spherical, nanorod and nanotube. The photocatalytic bactericidal action of NPs is size and shape dependent as discussed below. The comparison between the number of colonies growth after treatment with different bare NPs under UV irradiation at various time periods are listed in Table1.

Table 1. Comparison of bactericidal activity of different Bare TiO_2 nanoparticles

Nanoparticles	0 min	3 min	5 min	7 min	10 min	12 min	15 min
TiO_2 Spherical Bare 1mg	1500	1200	950	500	14	10	2
TiO_2 Nanorod Bare 1 mg	1500	950	400	203	86	2	0
TiO_2 Nanotube Bare 1 mg	343	295	247	119	3	0	0

With increase in the UV exposure time, the bacterial count was found to be decreasing in different extent by various shapes of TiO_2 and the complete killing of the bacteria was observed at nearly 15 min. The figure 6 below showed the graphical presentation of the comparative bactericidal activity of different shapes of TiO_2 nanostructures.

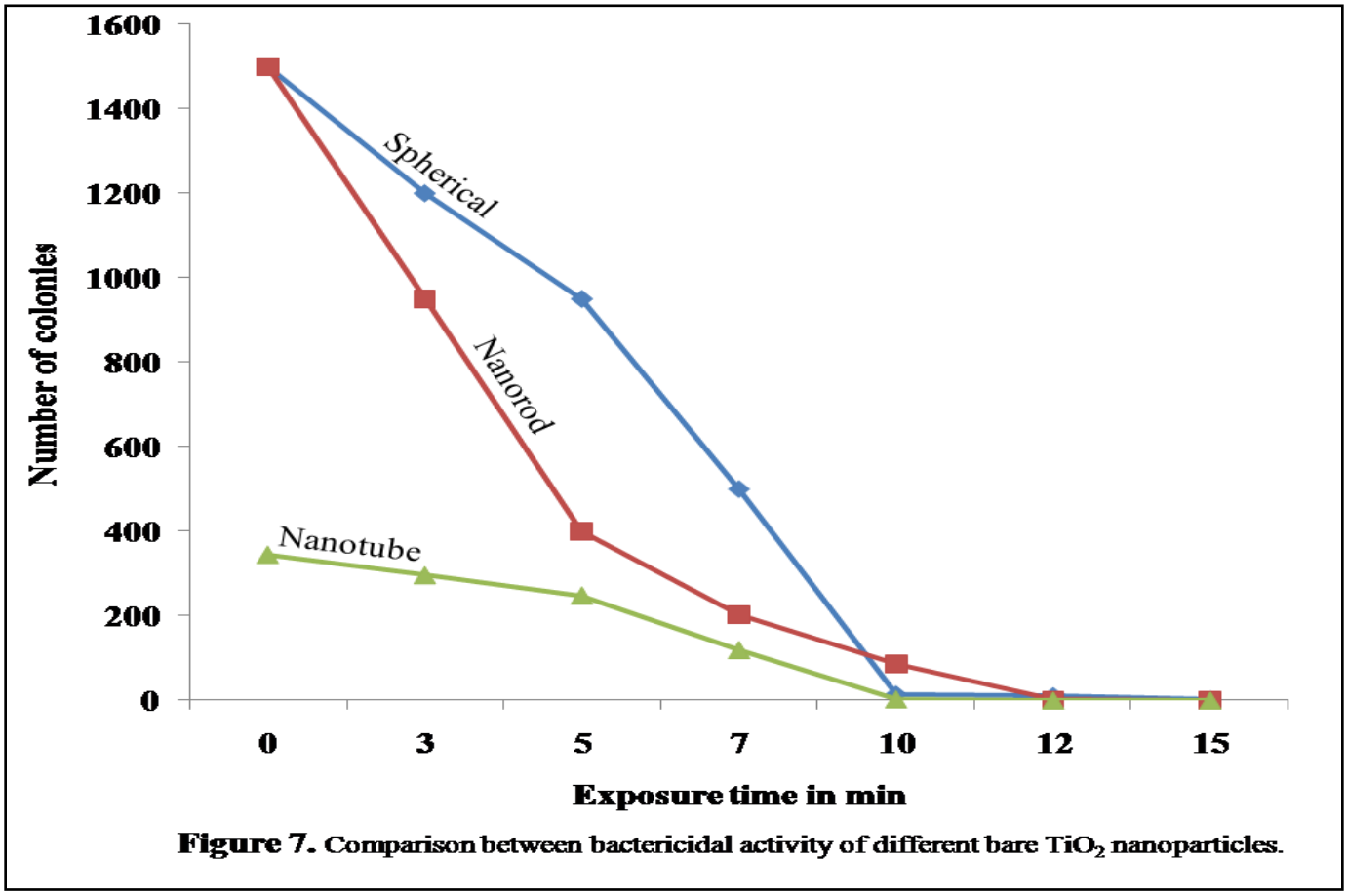

Figure 7. Comparison between bactericidal activity of different bare TiO_2 nanoparticles.

From the graph it is evident that the bacterial count decreased with exposure time in different extent due to unlike photoactivity of these photocatalysts. The bactericidal activity is different for different NPs at a particular time interval. As a whole nantubes are found to be more effective when compared to spherical and nanorods. The bacterial colonies formed after various times of UV irradiation over different shapes of TiO_2 NPs (1 mg) are shown in figure 8 below. From the figure it is clear that there is a large difference in the number of colonies between different NPs of dissimilar photoactivity because of their structural and surface morphological change which lead to modify the energetics of photoexcited charge species responsible for bacterial killing.

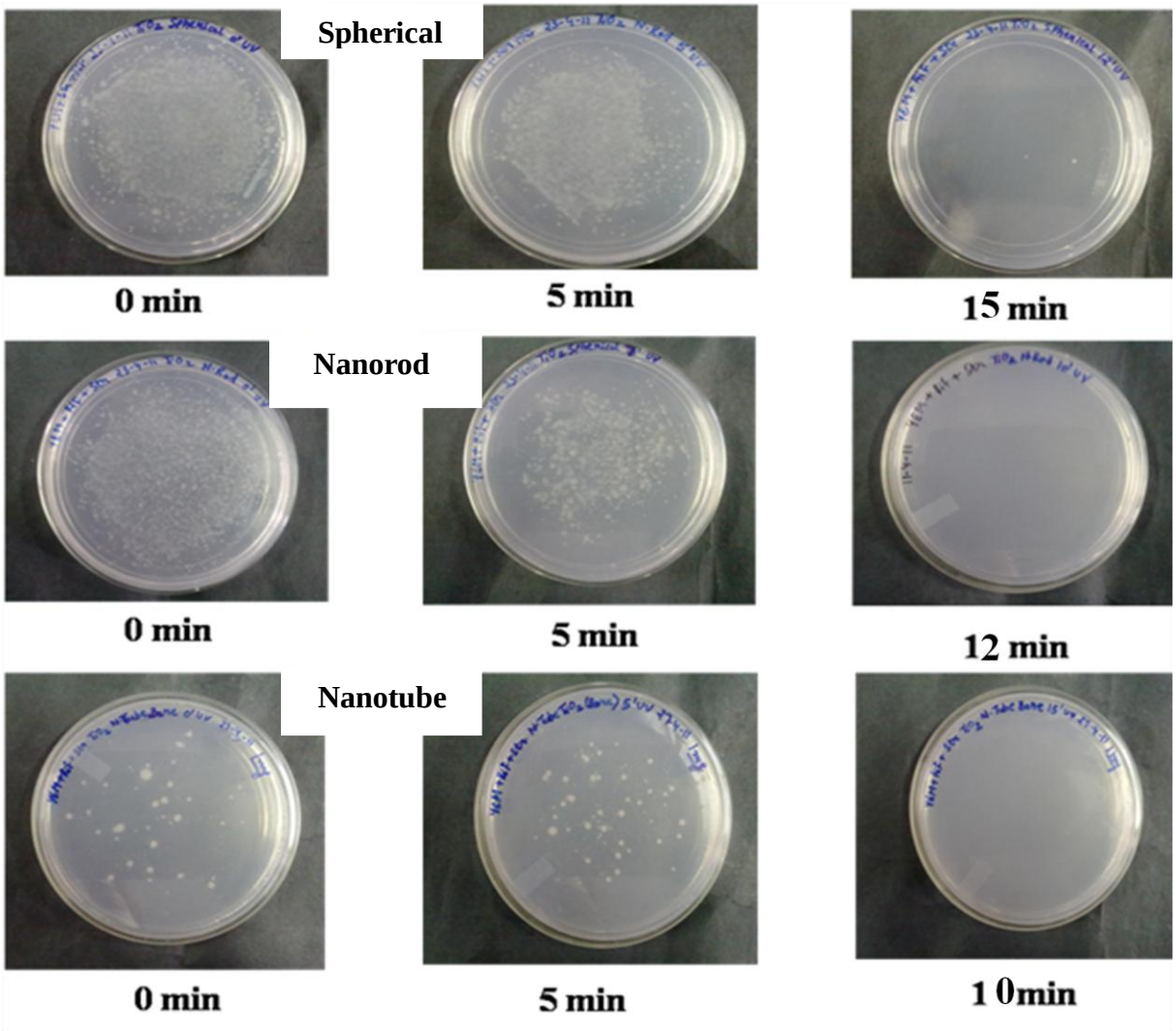

Figure 8. Bacterial colonies formed after UV irradiation of 1mg bare TiO_2 NPs at different time

5.3. Effect of Au, Ag and Cu loading on TiO_2 nanoparticles bactericidal activity

5.3 (i) Comparison between Bare and Metal loaded spherical TiO_2 nanoparticles on photokilling of bacteria

Table 2 below shows the comparative effect of the growth of bacterial colonies between bare and metal loaded TiO_2 under same experimental conditions. The bactericidal activity of bare and metal loaded spherical NPs was checked after irradiation of the bacterial suspension over glass slide containing 1 mg of bare and 0.5 mg of metal loaded TiO_2 spherical NPs.

Table 2. Difference in the number of bacterial colonies formed between bare and metal loaded spherical TiO_2

Nanoparticles	0 min	3 min	5 min	7 min	10 min	12 min
Spherical Bare 1 mg	1500	1200	950	500	14	2
Spherical Au 1 wt % (0.5m g)	925	686	197	5	0	0
Spherical Ag 1 wt % (0.5 mg)	0	0	0	0	0	0

Figure 9 shows that after 1 wt% Au and Ag loading bactericidal activity is highly improved and the growth of cell colonies are linearly decreased with irradiation time. The notable photokilling behavior of Ag loading means that Ag NPs have high antimicrobial property which is a proven fact and TiO_2 just enhanced this rate of bacterial death in shorter time of UV irradiation. The Au NPs do not have self biocidal activity hence, it is showing less activity due to only metal-TiO_2 effect. In the case of bare spherical NPs, complete killing was observed after a time interval of 12 min, where as in the case of Au loaded spherical NPs, complete photokilling was observed within 7 min of UV irradiation.

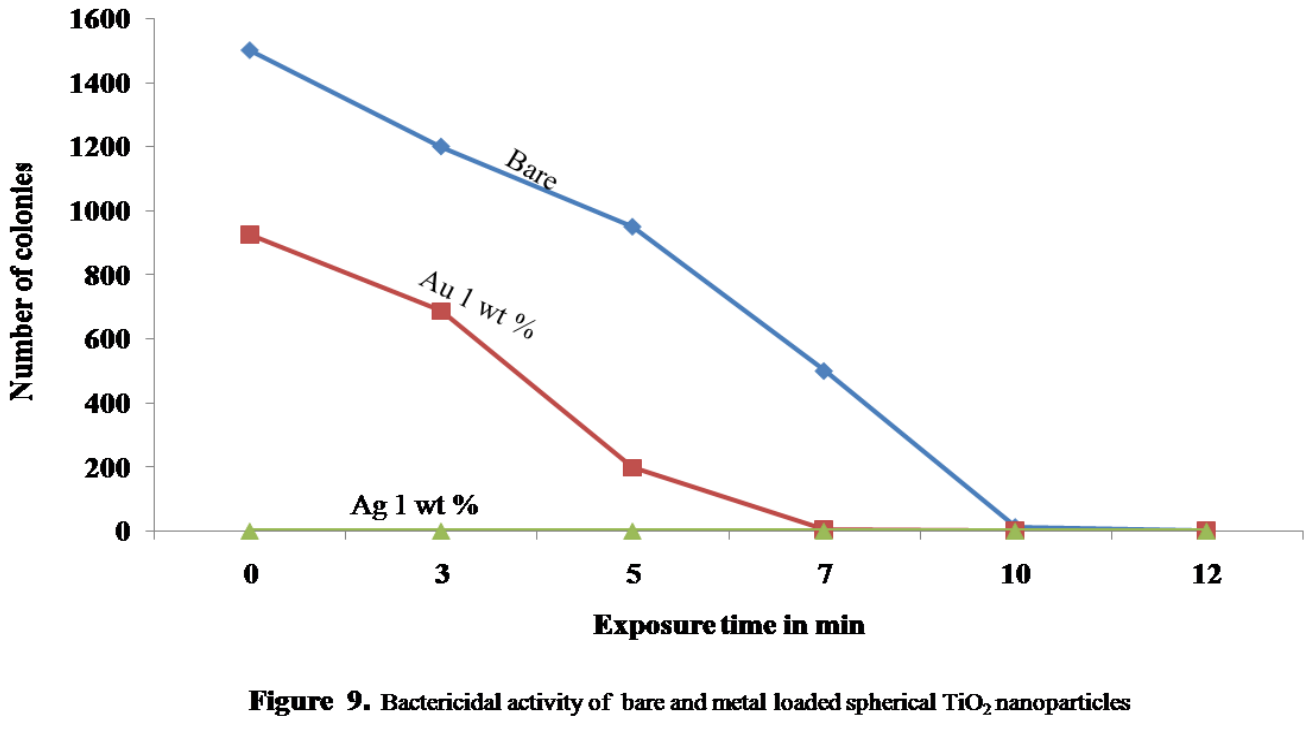

Figure 9. Bactericidal activity of bare and metal loaded spherical TiO_2 nanoparticles

From the above results, we can clearly say that metal loaded spherical TiO_2 NPs are more efficient in killing bacteria than bare NPs. These findings support the reports of the earlier observations as available in the literature. It is interesting to note that there are number of bacterial colonies (Figure 10) formed during control growth of initial cell concentration which is reduced to zero colony growth as soon as Ag-TiO_2 NPs are treated with the same cell suspension because of the high antimicrobial activity of bare Ag NPs only.

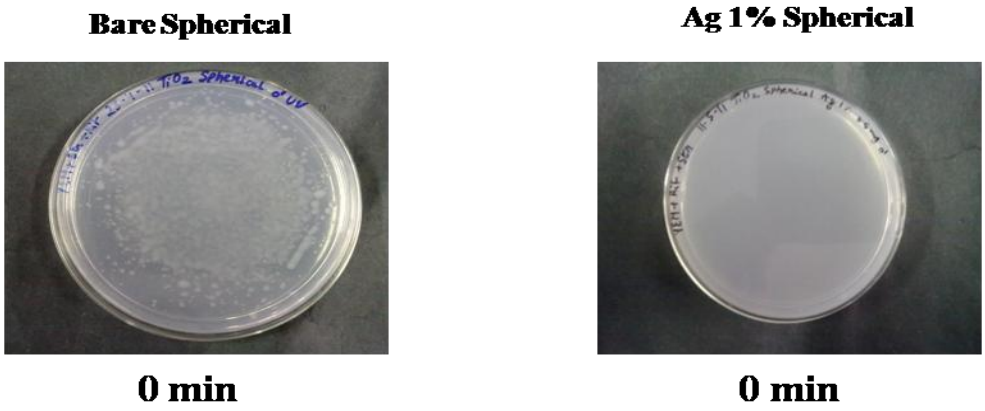

Figure 10. Bactericidal activity of 1 mg Bare and 0.5 mg 1% Ag loaded Spherical TiO_2 NPs

5.3 (ii) Comparison between Bare and Metal loaded nanorod TiO_2 on photokilling of bacteria

Similarly, the bactericidal activity of bare and metal loaded TiO_2 nanorods was checked after irradiation of the bacteria over glass slide containing 1 mg of bare and 0.5 mg of metal loaded TiO_2 nanorods. The comparison between the number of colonies formed after treatment with bare and metal loaded nanorods is listed in Table 3.

Table 3. Comparative bactericidal activity of bare and metal loaded TiO_2 nanotube

Nanoparticle	0 min	3 min	5 min	7 min	10 min	12 min	15min
TiO_2 N.Rod Bare 1 mg	1500	950	400	203	5	3	0
TiO_2 N.Rod Ag 1 wt % 0.5 mg	1200	470	389	234	119	0	0
TiO_2 N.Rod Au 1 wt % 0.5 mg	609	517	380	197	0	0	0

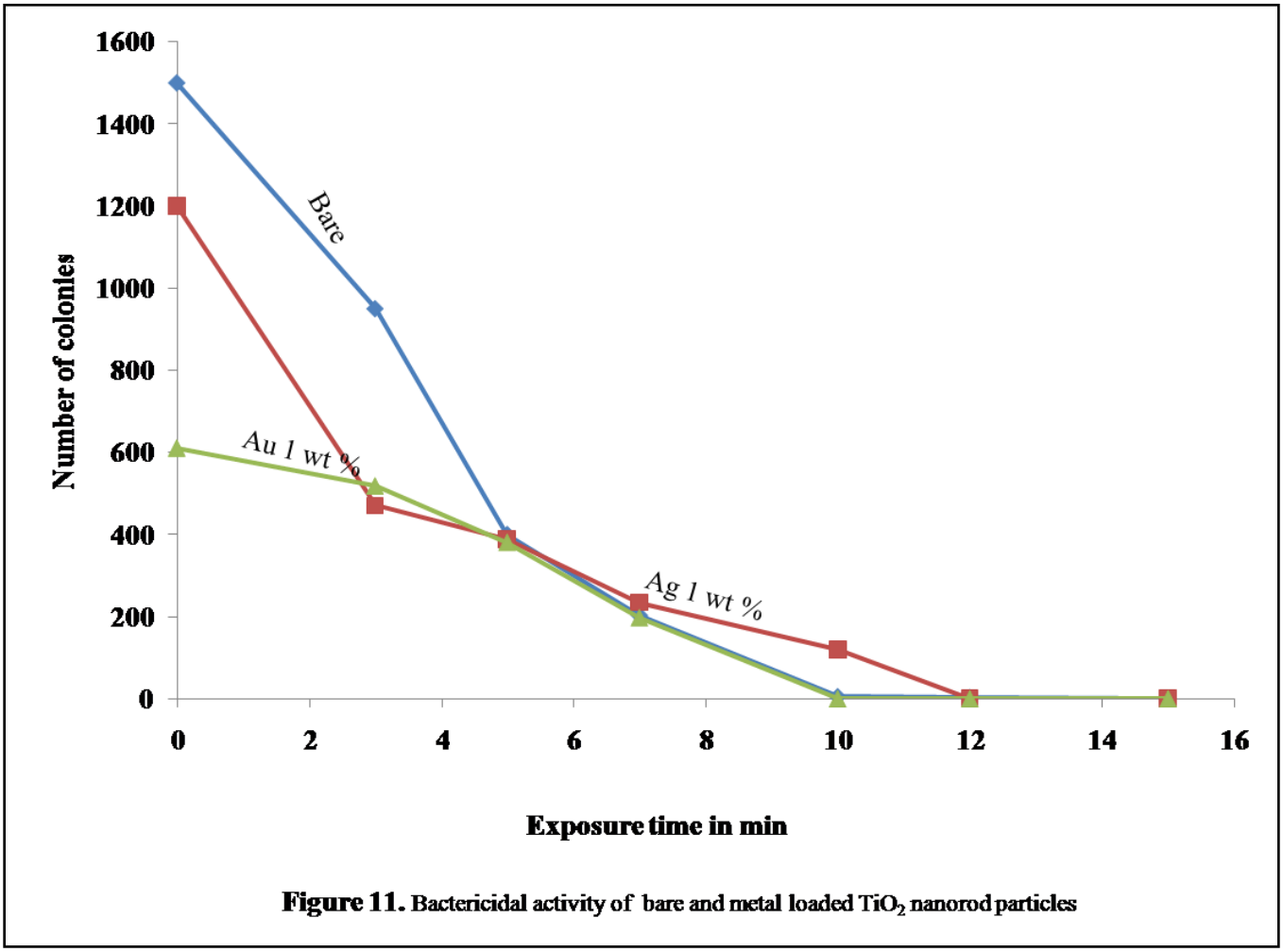

Figure 11. Bactericidal activity of bare and metal loaded TiO_2 nanorod particles

Figure 11 displays that the number of colonies decreased gradually in diverse extent with increase in the UV exposure over Au and Ag loaded TiO_2 nanorods. In the case of bare nanorods, photokilling was observed at a time interval of 15 min, where as in the case of 1wt% Ag and Au loaded nanorods, bacterial cell death was observed at 12 and 10 min irradiation. Figure 12 exhibits the growth of bacterial colonies after 10 min UV irradiation of 1 wt% Au and Ag loaded TiO_2 nanotube

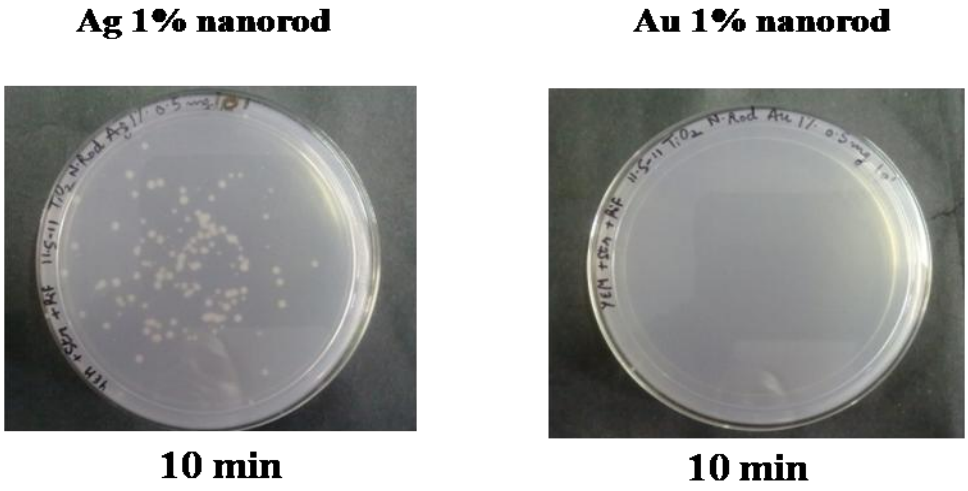

Figure 12. Bactericidal activity of Au and Ag loaded 0.5 mg TiO_2 nanorod particles.

5.3 (iii) Comparison between Bare and Coinage metal loaded nanotube TiO_2 on photokilling of bacteria

The bactericidal activity of 1 mg bare and 0.5 mg of 1wt% Ag, Au & Cu loaded nanotubes were carried out at different time intervals.

Table 4. Effect of Bare and metal loaded nanotube on bacterial photokilling

Nanoparticles	0 min	3 min	5 min	7 min	10 min	12 min	15min
TiO_2 Nanotube Bare 1mg	343	295	247	210	172	86	0
TiO_2 Nanotube Ag 1 wt % 0.5mg	0	0	0	0	0	0	0
TiO_2 Nanotube Au 1 wt% 0.5 mg	97	21	2	0	0	0	0
TiO_2 Nanotube Cu 1wt % 0.5 mg	510	476	305	167	0	0	0

The difference in the number of colonies between bare and metal loaded nanotubes after UV irradiation at different time intervals is listed in Table.4. It is clearly observed that metal loaded nanotubes are more effective in killing of bacteria than bare nanotubes.

From the graph in figure 13, it is further observed that 1 wt% Ag, Au & Cu loaded nanotubes exhibited different rates of bacterial photokilling as compared to the activity of bare nanotubes and the complete inhibition was observed at 0 min, 5 min and 10 min irradiation, respectively. Again Au and Ag loading significantly improved the bactericidal activity as compared to less reactive Cu loading because of their different co-catalytic activity.

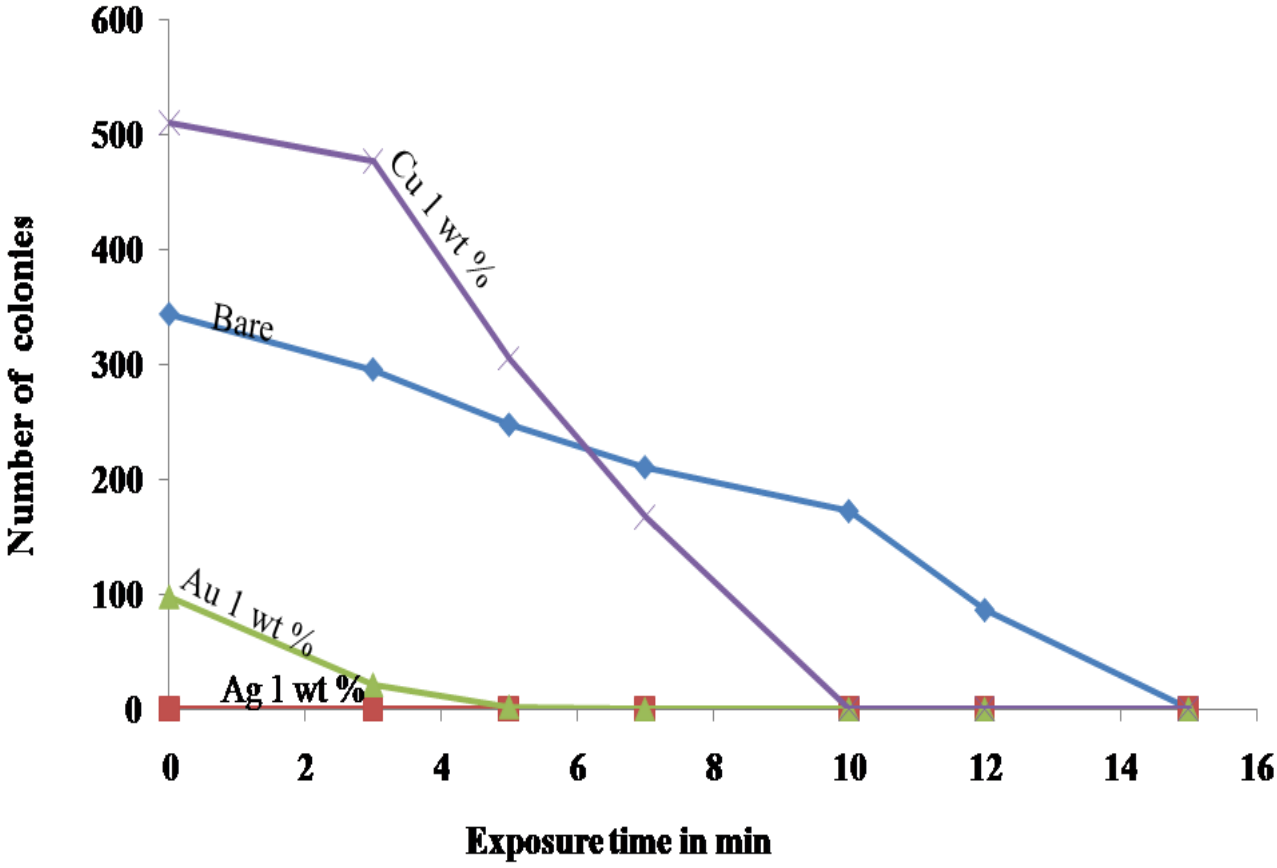

Figure 13. Bactericidal activity of bare and metal loaded TiO_2 nanotube particles

It is interesting to note that there is significant decrease in the bacterial count when treated with bare and metal loaded nanotubes. The 1 wt% Ag loaded nanotubes being more effective without any UV exposure followed by 1 wt% Au and Cu loaded nanotubes after 5 min and 10 min UV exposure, respectively. Figure 14 shows the difference in colony count after treatments with bare and metal loaded TiO_2 under constant, 5 min UV irradiation.

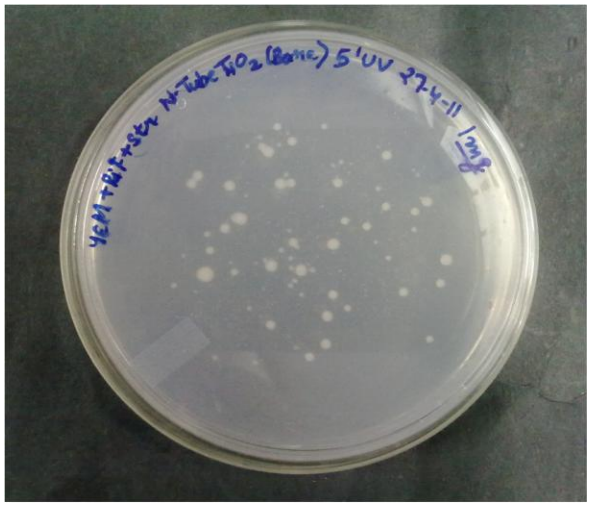

Nanotube bare -1 mg

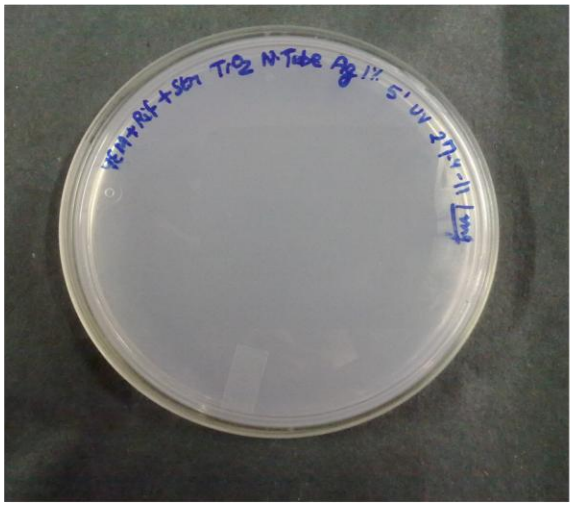

Nanotube Ag 1 wt %-0.5 mg

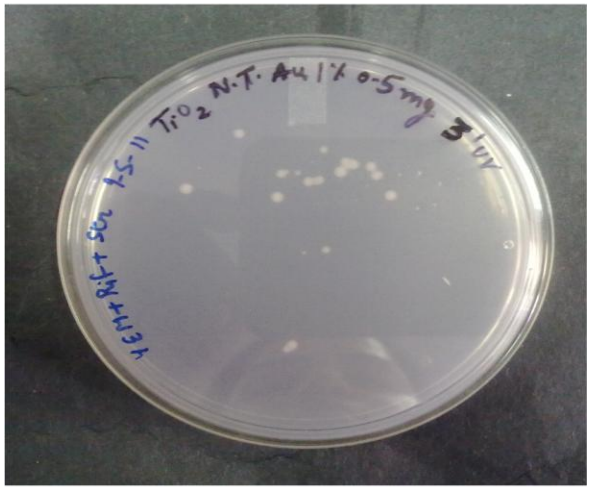

Nanotube Au 1 wt %-0.5 mg

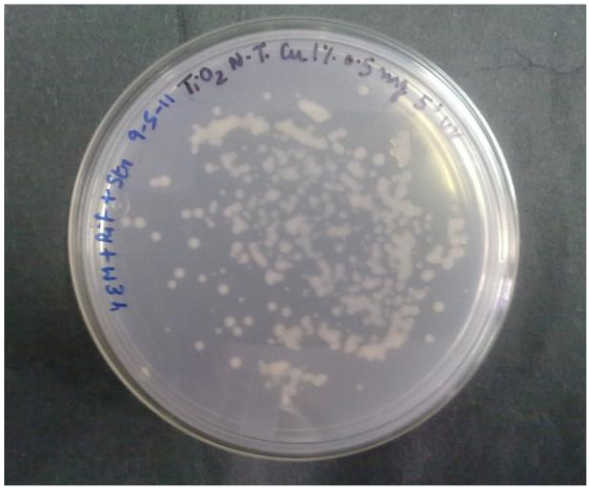

Nanotube Cu 1 wt %-0.5 mg

Figure 14. Bactericidal activity of Bare and metal loaded nanotube particles at 5 min UV exposure

5.3 (iv) Comparison between Au 1 wt % loaded spherical, nanorod and nanotube TiO_2 on photokilling of bacteria

As evident from figure 15 below, Au 1 wt % TiO_2 nanotubes are more effective in bacterial killing as compared to Au 1 wt % TiO_2 nanorods and spherical. This again can be attributed to high surface area of nanotube as compared to nanorod and spherical as metal loading is same in all the three cases.

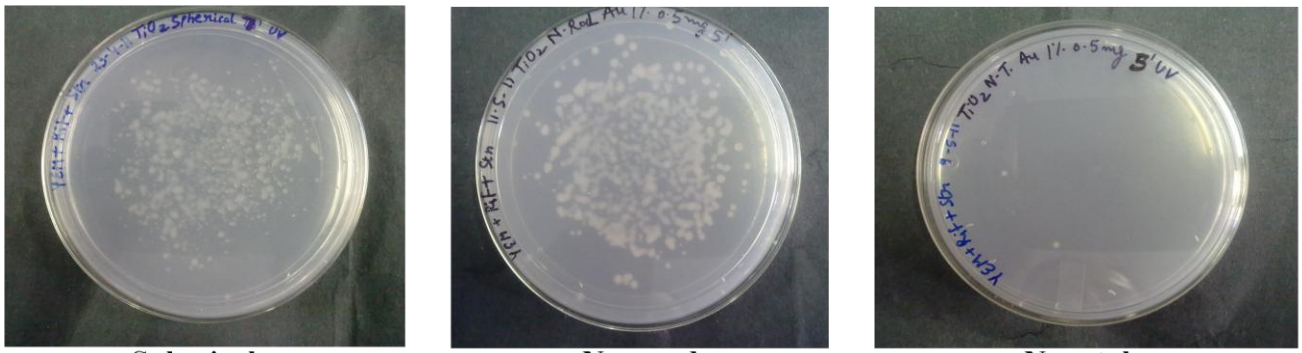

Spherical Nanorod Nanotube

Figure 15. Bactericidal activity of Au 1 wt % loaded TiO_2 particles at 5 min UV exposure

A clear difference in colony count can be seen between Au 1 wt% loaded nanotube and other shapes. Unlike Ag, Au itself does not possess any inherent toxicity it is the metal TiO_2 combined effect which is causing the bactericidal action in all the three cases (reducing the recombination rate of holes and electrons).

5.3 (v) Bar Graph showing bactericidal activity of all metal loaded TiO_2 nanoparticles

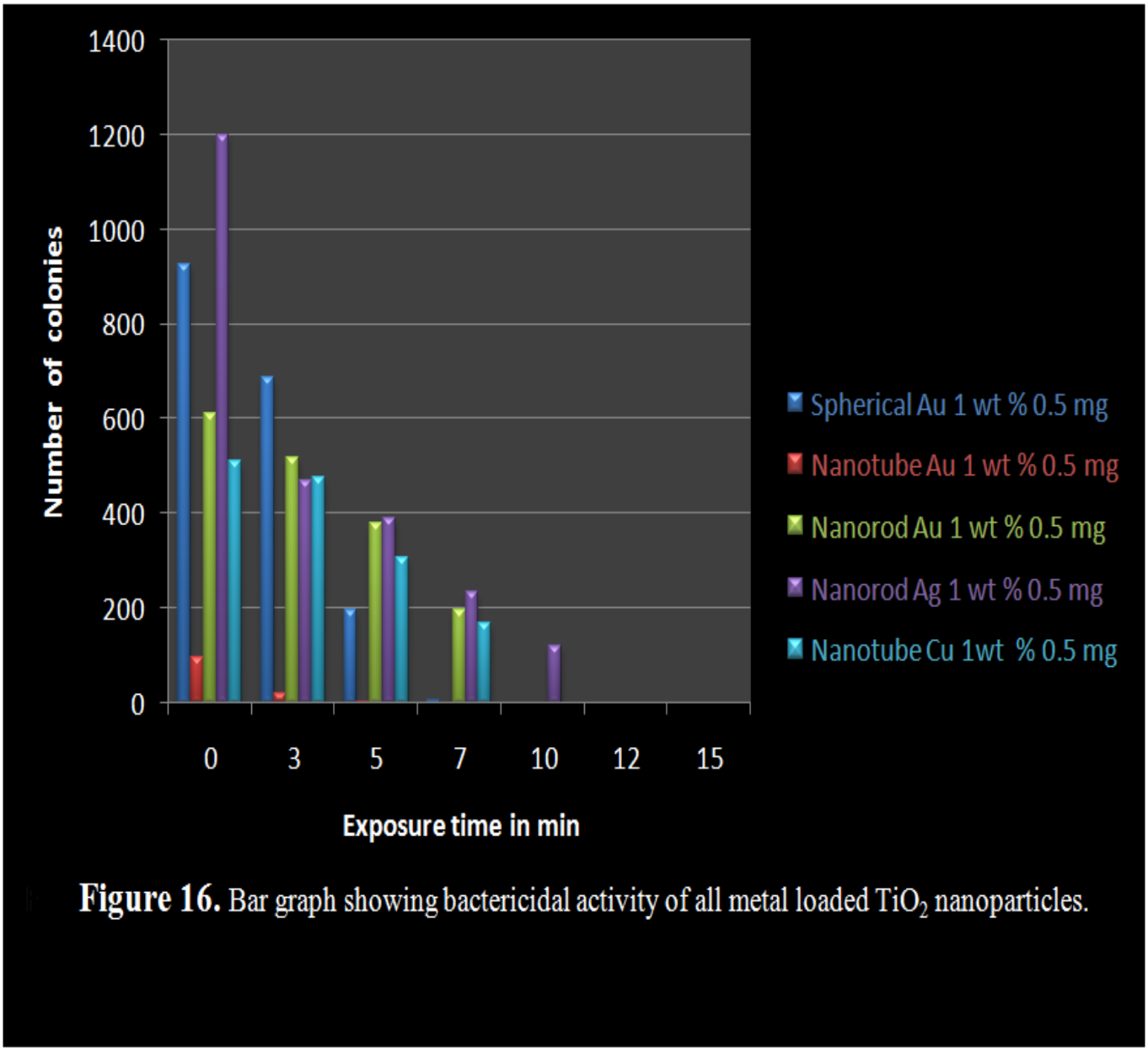

Figure 16. Bar graph showing bactericidal activity of all metal loaded TiO_2 nanoparticles.

Figure 16 shows that the bactericidal activity is different for different metal loaded TiO_2 NPs at a particular time interval and Ag loaded NPs are always found to be more effective due to its inherent biocidal activity as compared to Au and Cu loading.

5.4 Atomic Absorption Spectroscopy study

To ensure the bacterial decomposition, AAS was performed for analyzing the potassium ion leaching from the dead cells. The K^+ ions concentration was found to be 2.5 mg/l as compared to 0.4 mg/l of control (only bacterial culture, without the test sample and UV radiation). This

confirmed the destruction of bacterial cell wall, as K^+ is one of the main transport channels in any gram negative bacteria that are coming out after their photodecomposition.

It is assumed bacterial cells are killed due to the oxidative dissolution of the biochemical constituents of cell membrane by the highly oxidizing photogenerated holes and/ or hydroxyl radicals generated during light irradiation. This oxidation process of cell death for different shapes of TiO_2 can be explained on the basis of the varied rate of photogeneration of oxidizing holes in VB and unlike recombination rate of electron-hole pairs as a function of dissimilar surface to volume ratio, surface area and structural morphology. This oxidative photodegradation of intracellular chemical constituents (phospholipids, proteins and DNA etc.) leads to the decomposition of cell wall. As the TiO_2 particles and bacteria are stationary, the contact area of the cell surface is persistently photoetched and punctured by the attack of photoexcited holes or OH radicals during prolonged irradiation. As a consequence the cell wall is gradually damaged and eventually leads to structural and functional disorders of the cytoplasmic membrane that causes the cell death. A detailed kinetic analysis demonstrated that cell wall damage occurs in less than 20 min, followed by progressive damage of the cytoplasmic membrane and intracellular components. The Au, Ag and Cu deposition onto TiO_2 enhances the interfacial charge transfer rate by attracting conduction band electrons into Pt phase through Schottky–barrier electron trapping and retarding the electron (e^-) - hole (h^+) pair recombination. Therefore, accessibility of h^+ for the oxidizing reactions is greatly enhanced as compared to bare TiO_2. Also, metal nanodeposits could be beneficial by reducing the over potential of electron transfer to adsorbed oxygen and helps the generation of additional OH radicals along with water photooxidation by h^+ and initiate the oxidative reactions. An excellent linear correlation between *E. coli* bacteria death and OH radicals confirms that the OH radical is the primary oxidant species responsible for inactivating microbial cells. Finally, Atomic Absorption Spectroscopy analysis of potassium ion leakage from the dead bacterial cell was found to be 2.5 ppm in photoirradiated TiO_2 suspension compared to 0.4 ppm in control culture of without irradiation. Hence, it is clear that TiO_2 oxidizes the cell wall components leading to cell disruption and finally cell death.

6. Conclusion

The present findings prove the strong biocidal activity of Au, Ag and Cu-TiO_2 photocatalysts as compared to bare TiO_2 of various shapes. The size and shape effect of TiO_2 nanoparticles and nature of metal loading can influence electronic properties of the metal-TiO_2 composites as investigated by many researchers. Studies have revealed that metal-semiconductor composites exhibit shifts in the Fermi level to more negative potentials which is metal size-dependent. This shift enhances the charge transfer process in a different extent as a function of metal deposits and shape of TiO_2, resulting in the dissimilar activity of bare and various metal photodeposited TiO_2 photocatalysts of different shapes. It is found that drastic inactivation (within 10 min) of bacterial cells occur by low intensity UV exposure onto metal -TiO_2 suspension compared to longer contact time (> 30 min) as reported till date. The biocidal activity varied with the shape and nature of metal dispersion and their shape dependent energetics. We provide strong evidence for the vigorous photokilling of bacteria due to oxidative degradation of biomolecules present in bacteria. Therefore, the superior antimicrobial activity of metal photodeposition onto TiO_2 can be helpful in many applications. The self biocidal activity of bare Ag nanoparticles of desired size needs to be investigated for better knowledge about the photoexcited Ag-TiO_2 nanojunction**.**

7. References

A.S. Fauci, N.A. Touchette, G.K. Folkers. *Emerg. Infect. Dis.*, 11 (2005) 519-25.

I. Sondi, B.S. Sondi. *J. Colloid Interface Sci*., 275 (2004) 177–82.

Fresta, G. Puglisi, G. Giammona, G. Cavallaro, N. Micali, P. M. Furneri. *J. Pharm. Sci.*, 84 (1995) 895-902.

Hamouda, M. Hayes, Z. Cao, R. Tonda, K. Johnson, W.Craig, J. Brisker, J. Baker. *J. Infect. Dis,*. 180 (1999) 39-49.

W.A. Daoud, J.H. Xin, Y.H. Zhang. *Surf. Sci.*, 599 (2005) 69–75.

K. Ghule, A.V. Ghule, B.J. Chen, Y.C. Ling. *Green Chem*., 8 (2006) 1034–41.

S. Makhluf, R. Dror, Y. Nitzan, Y. Abramovich, R. Jelinek, A. Gedanken. *Adv. Funct. Mate.*, 15 (2005) 1708–15.

L. Qi, Z. Xu, X. Jiang, C. Hu, X. Zou. *Carbohydr. Res.*, 339 (2004) 2693–700.

A. E. Cubillo, C. Pecharroman, E. Aguilar, J. Santaren,J.S. Moya. *J. Mater. Sci.*, 41 (2006) 5208–12.

J.R. Morones, J.L. Elechiguerra, A. Camacho, K. Holt, J.B. Kouri, J.T. Ram´ırez, M.J. Yacaman. *Nanotechnology* 16 (2005) 2346–53.

A. Sclafani, L. Palaminisana, G. Marcı, A. Venezia. *Sol. Energy Mater. Sol. Cells.*, 51 (1998) 203.

J.C. Yang, Y.C. Kim, Y.G. Shul, C.H. Shin, T.K. Lee. *Appl. Surf. Sci.*, 121/122 (1997) 525.

J.C. Kennedy, A.K. Datye. *J. Catal.*, 179 (1998) 375.

A.L. Linsebigler, G. Lu, J.T. Yates. *Chem. Rev.*, 95 (1995) 735.

M.R. Hoffmann, S.T. Martin, W. Choi, D.W. Bahnemann. *Chem. Rev.*, 95 (1995) 69.

A. Hagfeldt, M. Gratzel.*Chem. Rev.*, 95 (1995) 49.

M.A. Fox, M.T. Dulay. *Chem. Rev.*, 93 (1993) 341.

D.M. Blake, J. Webb, C. Turchi, K. Magrini. *Sol. Energy Materials.*, 24(1991) 584.

P.V. Kamat. *Chem. Rev.*, 93 (1993) 267.

J.B. Neiland. *Ann. Rev. Microbiol*., 36 (1982) 285.

D.C. Borg, K.M. Schaich. Ed., B. Halliwell. *Fed. of Am. Soc. For Exp. Bio.*, (1988) 206.

R.J. Youngman. *Trends in Biochem. Sc*., 9 (1984) 280.

T. Matsunaga, R. Tomoda, T. Nakajima H. Wake. *FEMS Microbiol. Lett.*, 29 (1985) 211-214.

T. Matsunaga, R. Tomoda, T. Nakajima, N. Nakamura, T. Komine. *Appl. Environ. Microbiol.*, 54 (1988) 1330-1333.

M. Cho, H. Chung, W. Choi, J. Yoon. *Appl. Environ. Microbiol.*, 71(2005) 270-275.

M. Cho, H. Chung, W. Choi, J. Yoon. *Water Res.*, 38(2004)1069-1077

P.-C. Maness, S. Smolinski, D. M. Blake, Z. Huang, E. J. Wolfrum, W. A. Jacoby. *Appl. Environ. Microbiol.,* 65 (1999) 4094-4098.

S. Banerjee, P. J. Gopal, P. Muraleedharan, A. K. Tyagi, B. Raj. *Curr. Sci.,* 90 (2006) 1378-1383.

C. Mccullagh, J. C. Robertson, D. W. Bahnemann, P. K. J. Robertson. *Res. Chem. Intermed.,* 33 (2007) 359-375.

K. Sunada, T. Watanabe, K. Hashimoto. *J. Photochem. Photobiol. A: Chem.,* 156 (2003) 227-233.

G. Rincón, C. Pulgarin .*Appl. Catal. B: Environ.,* 44 (2003) 263-284.

X. Zhang, H. Su, Y. Zhao, T. Tan. *J. Photochem. Photobiol. A: Chem.,* 199 (2008) 123-129.

C. Hu, J. Guo, J. Qu, X. Hu. *Langmuir,* 23 (2007) 4982-4987.

C. C. Trapalis, P. Keivanidis. *Thin Solid Films*, 433(2003) 186- 190.

S. Pal, Y. K. Tak, J. M. Song. .*Appl. Environ. Microbiol.,* 73(2007)1712- 1720.

L. Armelao, D. Barreca, G. Bottaro, A. Gasparotto, C. Maccato, C. Maragno, E. Tondello, L.Stangar, M. Bergant, M. Mahne. *Nanotechnology* 18(2007) 375-709.

G. R. Bamwenda, S.Tsubota, T. Nakamura, M. Haruta. *J. Photochem. Photobiol. A: Chem.,* 89 (1995) 177-189.

B. Ohtani, K. Iwai, S. -I. Nishimoto, S. Sato. *J. Phys. Chem. B,* 101 (1997) 3349-3359.

P. Pichat, M. N. Mozzanega, J. Disdier, and J. M. Herrmann. *New J. Chem.,* 6 (1982) 559–564.

C. Sungbom, M. Kawai, K. Tanaka. *Bull. Chem. Soc. Jpn.,* 57(1984) 871-872.

J. Lee, W. Choi. *J. Phys. Chem. B*, 109 (2005) 7399- 7406.

M. C. Hidalgo, M. Maicu, J. A. Navı´o, G. Colo´n. *Catal Today*, 129 (2007) 43-49.

G. Bamwenda, S. Tsubota, T. Nakamura, M. Haruta. *Catal. Lett.,* 44 (1997) 83-87.

Z. Huang, P. -C. Maness, D. M. Blake, E. J. Wolfrum, S. L. Smolinski, W. A. Jacoby. *J. Photochem. Photobiol. A: Chem.*,130 (2000) 163-170.

N. Huang, Z. Xiao, D. Huang, C. Yuan. *Supramol. Sci.,* 5 (1998) 559-564.

V. Subramanian, E. E. Wolf, P. V. Kamat. *J. Am. Chem. Soc.,* 126 (2004) 4943- 4950.